Nuclear Inst. and Methods in Physics Research, A 1025 (2022) 166028

Contents lists available at ScienceDirect

Nuclear Inst. and Methods in Physics Research, A

journal homepage: www.elsevier.com/locate/nima

Experimental characterization of the internal ion source for the AMIT compact cyclotron

Pedro Calvo *, Diego Obradors *, Rodrigo Varela, Iván Podadera, Concepción Oliver, Antonio Estévez, Manuel Domínguez, Cristina Vázquez, Fernando Toral, Luis García-Tabarés, José Manuel Pérez

Department of Technology, Centro de Investigaciones Energéticas, Medioambientales y Tecnológicas (CIEMAT), Madrid, Spain

ARTICLE INFO

Keywords:
PIG-type ion source
Negative hydrogen ions
Discharge characteristic
Compact cyclotron

ABSTRACT

The ion source is one of the most relevant elements in a cyclotron, since it determines the injection into the accelerator. An internal cold-cathode Penning ion source has been chosen for the AMIT compact cyclotron. This kind of source is extensively used in cyclotrons to produce negative hydrogen ions. The compactness of the accelerator constrain the beam diagnostic in the cyclotron, motivating the development of an external experimental facility for the commissioning of the ion source. In this paper, the validation of the ion source design and the characterization of the H^- beam production are presented. Different chimney geometries modifying the distance between the plasma column and the extraction wall have been tested to obtain the best relation between ion production and plasma conditions. In addition, experimental measurements of the beam profile have been carried out. Current experimental results provide relevant information for the operation in the final cyclotron assembly and the final beam current optimization.

1. Introduction

The use of radioisotopes for nuclear imaging techniques, especially Positron Emission Tomography (PET) short life isotopes, has increased considerably over the past few decades [1]. Therefore, the current centralized medical isotope production and supply system must be adapted to the needs of society [2–4]. For that purpose, a ground-breaking compact superconducting cyclotron, AMIT, has been developed by CIEMAT and commercialized by Cyclomed Technologies [5].

The cyclotron is aimed at the production of single doses of ^{18}F and ^{11}C radioisotopes in a optimized size design. It will contribute to the deployment in hospitals for an on-site radioisotope production that will reduce the corresponding delivery costs. A suitable production of the selected radionuclides entails a beam requirements of 10 μA beam of 8.5 MeV protons at the target [6]. AMIT cyclotron, based on a weak focusing concept, employs two superconducting coils of NbTi in a Helmholtz arrangement to provide the 4 T magnetic field in a warm iron configuration [7]. The magnet is cooled down with two-phase helium, circulating in a closed circuit and re-condensed externally in a ground-breaking Cryogenic System Supply [8]. The radio-frequency system [9] consist of a 180° Dee attached to the cavity, with a 60 kV accelerating peak voltage imposed by the non RF-particle isochronism. In order to contribute to the high compactness of the accelerator, a cold-cathode Penning Ionization Gauge (PIG) ion source has been developed to produce a H^- beam that will be extracted from the accelerator through stripping-based system. The simplicity of this kind of source makes it the most common solution for cyclotron used for short-life radioisotope production.

The performance of the ion source plays a relevant role in the final operation of the cyclotron. It allows optimizing the beam current injected and the vacuum level inside the acceleration chamber, connected, likewise, with the beam losses by interaction with the residual gas. However, the compactness of the accelerator imposes restrictions on the beam diagnostics available during commissioning and operation of the accelerator, disabling the performance characterization of the source. Therefore, testing the ion source in a stand-alone facility becomes a relevant feature for optimizing the radioisotope production. Different ion source test facilities for cyclotrons have been worldwide developed [10–14]. A novel Ion Source Test bench facility (IST) has been designed, constructed and commissioned at CIEMAT in order to study the discharge characteristics and improve the ion source efficiency of the AMIT cyclotron.

* Corresponding authors.
E-mail addresses: pedro.calvo@ciemat.es (P. Calvo), diego.obradors@ciemat.es (D. Obradors).

https://doi.org/10.1016/j.nima.2021.166028
Received 23 November 2020; Received in revised form 8 November 2021; Accepted 14 November 2021
Available online 17 December 2021

2. Experimental setup

2.1. Ion source

The AMIT ion source consists of two cathodes and a hollow anode cylinder, usually called chimney, with an aperture for beam extraction. The cathodes are made of Tantalum due to the high thermionic emission current density, the high melting point and the high mechanical strength. The anode is made of copper–tungsten alloy, because of suitable thermal properties and good machining qualities. The slit size is 6 mm height and 0.2 mm width with 0.1 mm thickness to increase the penetration of the electrical field of extraction and keeping enough thickness to avoid a quick erosion due to the sputtering. The anode is held between two hollow copper blocks which are water cooled, where the cathodes are accommodated. A detailed scheme of the ion source specifying the different components is shown in Fig. 1, whereas Fig. 2 shows real pictures of the source.

The ion production begins to be relevant with the thermionic electron emission by the cathodes. The hydrogen gas injected directly into the source through the cathodes cavity is ionized, generating a plasma. In the anode volume, the production of negative hydrogen ions is primarily determined by the equilibrium between the creation and destruction processes through different reactions [15–17] between gas molecules, ions and electrons, depending on the energy of the electrons.

The low binding energy of H^- (<1 eV [18]) allows the secondary electron to be easily stripped by collisions with high-energy electrons. Therefore, H^- ions survive mainly on the outer shell of the plasma column, where the energy of electrons is lower. To compensate for the destruction channel, the design of the ion source enhances the production and survival of the H^- in the plasma by the implementation of an expansion gap of 0.3 mm between the plasma column boundary and anode slit wall, a region where there are cold electrons about few eV and fast electrons are excluded.

2.2. Ion Source Test facility

The objectives of the Ion Source Test facility are to validate and optimize the design of the ion source and characterize its operation, performing experimental measurements to determine the optimal operating conditions of the ion source, as well as the characterization of the resultant beam [19]. The measurements are taken with beam diagnostics focused on electrical measurements of the extracted beam, depending on the operational parameters of the source, the geometry of the system and the extraction conditions. During the operation, the arc current, the arc voltage, the gas flow, the vacuum pressure, the magnetic field and the extraction voltage are monitored and recorded. All these parameters influence on the internal performance of the ion source as well as on the extracted beam.

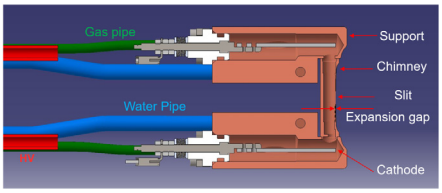

Fig. 1. Cross section of the ion source where the main elements are identified.

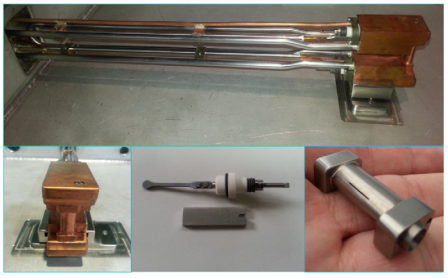

Fig. 2. Pictures of the ion source showing a lateral view with the water cooling pipes and the gas supply pipes (top), a frontal view of the main body of the source and the anode (bottom left), a cathode with electrical insulator (bottom center) and the chimney (bottom right).

The IST (Figs. 3 and 4) consists of a mechanical structure that holds a vacuum chamber where the ion source is introduced. The chamber is designed to be introduced inside a warm dipole magnet. It produces the magnetic field necessary to generate the operating conditions of the source as well as to bend the beam out the ion source. The IST magnet is a dipole with a cylindrical pole and copper coils providing a maximum field of 0.86 T. A 3D optimization of the electromagnetic design was performed, which was later manufactured by the company ANTEC [20].

The ion source generates charged particles by an electric discharge applied by the Ion Source Power Supply (ISPS) to the cathodes, generating a plasma by electron induced ionization of the hydrogen gas. The plasma is confined by the external orthogonal magnetic field. An electrical shielded box is installed inside the vacuum chamber with a devoted puller mechanism, which fixes an extraction gap during operation of 3 ± 1 mm. A positive DC high-voltage is applied to the box to extract the negative particles from the ion source, which is grounded. This high-voltage system allows the validation of the ion source with a technically simple facility. The electrical box shields the electric field like a Faraday cage and therefore the trajectories of negative ions inside are unaffected by any accelerating field. However, the beam path can be modified during the operation by the external magnetic field, tuned by the applied current to the coils. The gas handling system Bronchorst model controls the flow rate of hydrogen into the source in a range of 0 to 10 sccm (±0.06 sccm). To achieve a low stripping losses rate as well as a rapid pumping speed, the vacuum system uses two diffusion pumps of 1300 l/s and one rotary vane vacuum pump of ∼40 m^3/h. A schematic overview of the ion production in the facility is illustrated in Fig. 5.

The IST facility includes several interceptive beam diagnostics for an optimum characterization. On the one hand, the total beam current generated is measured with some beam probes which can be located at three different positions, two of them with a fixed structure and the third with a movable system by a piezoelectric motor to provide variable measurements. The current is measured with a picoammeter, adjustable in different ranges of measures with associated error of 0.6%. On the other hand, the transverse beam profile can be measured through a Al_2O_3:Cr fluorescent screen [21].

The versatility of the IST facility has additionally allowed to test and verify some other subsystem of the AMIT cyclotron beyond the ion source. The vacuum system, the beam diagnostics, the water cooling system and the operational control system among other minor elements have been tried and tested.

3. Results and discussion

The final objective of the experimental measurements of the ion source is focused on verifying the ion source design and its adequate operation under the control parameters and establishing the achievable beam current range in order to meet the cyclotron beam requirements. Therefore, the ion source parameters influence must be perfectly characterized to satisfy an adequate beam current injection during the cyclotron operation.

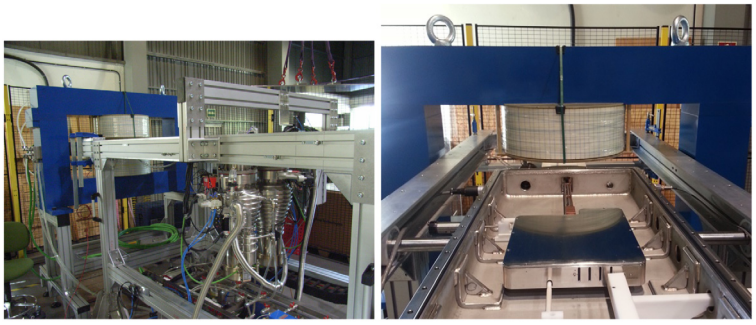

(a) (b)

Fig. 3. Ion source test facility. (a) Overview of the test bench with the mechanical structure, the magnet, the vacuum system and the refrigeration water distribution system. (b) A top view inside the vacuum chamber, showing the electrical shielded box, the ion source and the magnet.

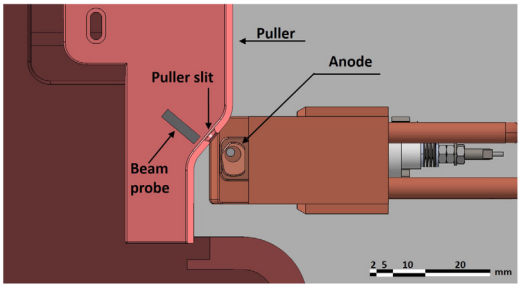

Fig. 4. Schematic top view of IST showing the beam extraction region from the ion source and the beam probe inside the electrical shield box.

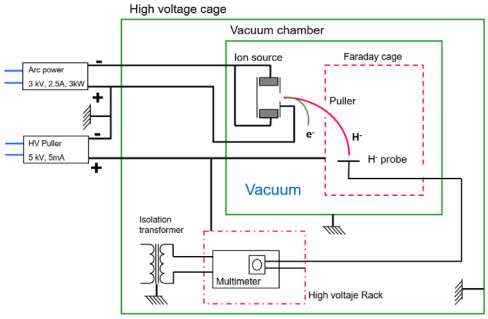

Fig. 5. Diagram of ion source operation at the IST.

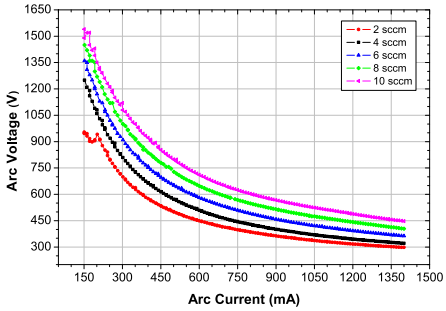

Fig. 6. Arc voltage in front of arc current with a magnetic field of ~0.5 T (I_{coil} = 135 A).

3.1. Ion source performance

The experimental performance operation of a cold cathode PIG ion source is determined by the plasma properties. The plasma resistivity [22] is defined as:

$$\eta = \frac{m_e \nu_e}{e^2 n_e} \tag{1}$$

where m_e is the electron mass, n_e is the electron density and ν_e is the Maxwellian-averaged electron–ion collision frequency of binary collisions that depends on ion density and temperature. The plasma inside of the ion source can be considered as an equivalent electric circuit. Thus, as a first approximation, the DC arc voltage and current are related with the resistance according to Ohm's law, and therefore with the resistivity and the internal geometry of the chimney.

The ion source operation requires the presence of a magnetic field parallel to the chimney axis. Electrons emitted from either cathode are accelerated by the potential difference between the cathode and the anode. Their movement is along expanding helical orbit crossing the hollow anode and proceed toward the opposite cathode due to the axial magnetic force. The neutral gas injected is ionized, generating a plasma which is confined by the magnetic field. The cathodes are self-heated by back accelerated ionic bombardment, that it is supplied by plasma ionization process.

The pure penning discharge can also be driven into an arc discharge by increasing the gas flow of a source already at high voltage; this is referred to as "striking the arc", and is generally the main way in which the arc discharge is initiated to start the hydrogen breakdown. As the gas pressure is increased, the current increases, the cathodes heat up and begin to supply electrons by thermionic emission. This increases the current with further cathode heating until the current is limited by the external circuit. The transition to full thermionic operation can be clearly seen and it will not occur below a critical pressure. The minimum pressure at which the transition occurs and the impedance of the source are determinate by the heat conduction of the cathode stems. Lower heat conduction results in higher cathode temperature and a lower arc impedance and voltage for a given current. Thus, by varying the pressure, the arc voltage can be controlled for a given current. The standard behavior of the source in this stage is described by the decrease of the arc voltage while the arc current is increased, as it is illustrated in Fig. 6. The experimental error associated with the ion source parameters is due to the systematic uncertainty of the acquisition system measurements, being 0.5% for arc current measurement and 0.05% for voltage.

The characterization of the ion source according to the gas flow rate is illustrated in Fig. 7. As the initial flow rate increases, more molecules are available for plasma production and the resistance decreases, causing a slight decline of the arc voltage. As the gas flow raise further, the drift velocity of the charged particles is reduced, the electron collision frequency increases and the plasma resistance increases. Furthermore, modifications in the plasma density produce variations in the ionization probability as well as in the probability of recombination for charged particles due to the adjustment of electron mean free path. Thus, these

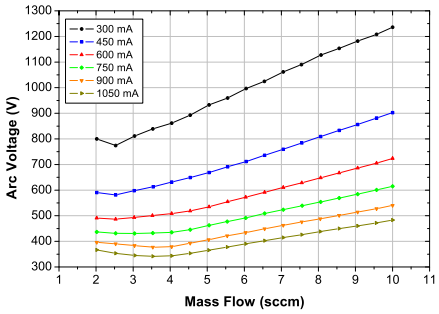

Fig. 7. Arc voltage as a function of the gas flow at different arc currents. This measurement is taken with a magnetic field of ~0.5 T (I_{coil} = 135 A).

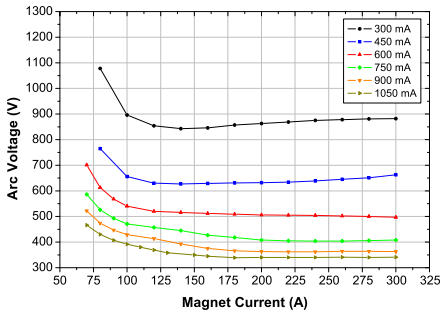

Fig. 8. Arc voltage as a function of magnet coil current at different arc current (4 sccm of gas flow rate).

two effect affecting to the plasma resistivity compete with each other while the gas flow rate changes.

The magnetic field is other parameter to consider because it modifies the trajectory of the charged particles in the plasma and consequently, it affects to the averaged electron–ion collision frequency. However, their influence is of less relevance due to the volume of the plasma is small and the internal pressure is high. Thus, the plasma conditions remain almost unchanged against variations of the magnetic field as long as it reaches certain value that evince the stability of the plasma (Fig. 8).

3.2. Beam current measurements

The produced beam is directly related to plasma status and the extraction conditions, specifically the electric field that depends on the applied voltage and the puller–ion source distance. The electric field penetrates through the slit of the ion source, extracting negative charged particles from the plasma. The electrons are bent by the magnetic field with small radii compared with that of the ions, due to their tiny mass, and they collide outside of the source. H^- ions are transported from the ion source into the electric shield box where they are collected by a fixed beam probe located at the entrance of the cage.

The extracted current from a charged particle source has two different regimes as a function of the extraction voltage [14]. The first is the so-called space-charge (SC) limited emission regime. In the SC-regime the electron beam emission is limited by the beam itself. This leads to reduced emission of the cathode because the space charge of the particles already emitted compensates the extraction field, making it impossible to extract a higher current density. The maximum current density, J, can be calculated by the Child–Langmuir law [23,24]:

$$J = \frac{4\sqrt{2}}{9}\,\varepsilon_0\sqrt{\frac{q}{m}}\,\frac{V^{3/2}}{d^2} \tag{2}$$

applied to parallel plates surfaces, where V is the applied extraction potential and d is the separation between the extractor and the emission surface. From this equation, the ratio between current and extraction voltage, called the beam perveance, can be deduced:

$$P = \frac{I}{V^{3/2}} \tag{3}$$

It is the proportionality constant that describes the extraction system. It refers to the strength or ability of the plasma to deliver ions. For a specific charged particle, the perveance only depends on the geometry. As long as the emission is space-charge-limited, the perveance is roughly constant. When the voltage is further increased and the beam emission is no longer space-charge-limited, the beam perveance decreases.

As extraction voltage is increased, the extracted current density saturates by the emission limit of the plasma. Then, the ion source starts to emit in the production-limited emission according to the thermionic regime, which is the heat-induced flow of charge carriers from a surface or over a potential-energy barrier.

The H^- beam current has been measured at IST as a function of different DC extraction voltages. The high voltage of the puller is restricted to reduce HV breakdown phenomena due to the excessive spark occurring in the space between the extractor and the ion source. To diminish this effect, a resistor was placed between the high voltage power supply and the extractor. Therefore, all measurements are referenced with respect to the effective voltage in the electric shield box. The results (Fig. 9) manifest the transition in the operating regime of ion production. First the space-charge limited emission is dominant and above a certain extraction voltage the current extracted from the plasma is limited by the production emission. The curve fitted to the data in Fig. 9(b) shows that the perveance of the AMIT internal ion source during the space-charge limited emission is $P \simeq 0.1$–0.5 mA kV$^{-3/2}$, according the ion source conditions. Whereas in the production emission regime, the current extracted increases slowly for higher voltages with an approximate slope of 10–45 μA/kV according to the plasma properties.

The beam current extracted from the ion source can be increased by modifying on the plasma density conditions through the arc discharge current and the gas flow rate. The high interdependence between the different magnitudes plays a fundamental role in the optimization of the ion source, allowing the tuning of the beam extracted current through different control parameters of the ion source. Regarding the arc current, during the operation of the cyclotron, it must be adjusted so that the final current at the target fulfills the beam requirements (10 μA). Once this condition is satisfied, the arc current should be minimized to reduce secondary losses, wear and tear of the cathodes and the consequent economic and material costs.

The dependence between the extracted beam current of H^- with respect to the gas flow rate comes from the particle interaction reactions in the plasma. As the gas load increases, a greater number of ionization occurs for a given arc current, but electrons with adequate energy for production are limited and the high pressure inside the chimney decreases the survival of H^- ions. In addition, other processes such as insufficient supply of gas molecules, the increase percentage of neutral particles that are positively ionized, the excess supply of electrons with destructive energy and the neutralization rate must be taken into account.

The results presented in Fig. 10 show how the variation of the gas flow rate at fixed arc current provides a quickly increase of the beam current until a value around 4 sccm, which saturate the balance between ion production–destruction reactions. Therefore, this value can be considered optimal for the operation of the ion source, since it maximizes the H^- current generated, minimizing the gas load and consequently the vacuum level in the chamber, a relevant factor in the beam losses by interaction with the residual gas.

It is also important to consider that there are other factors that influence the H^- production, although with less relevance, such as the magnetic field, the vacuum chamber pressure, the extraction gap distance, the chimney–puller alignment, the internal geometry of the chimney... Those factors can provoke the non-repeatability of the factor values

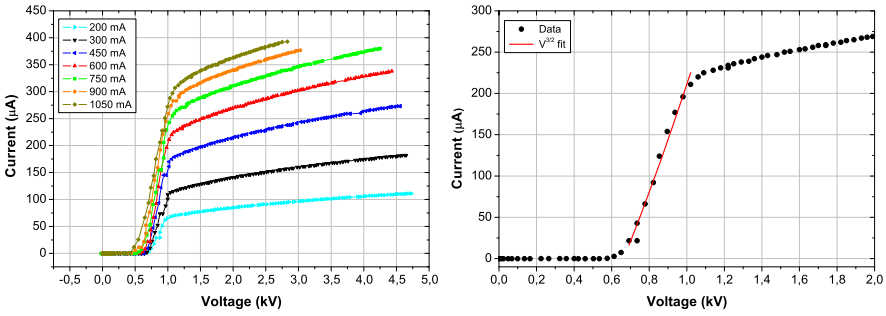

(a) (b)

Fig. 9. (a) Beam current measurement at the beam probe in front of the effective extraction voltage for different arc current with a fixed gas of 4 sccm an magnetic field of ∼0.5 T (I_{coil} = 135 A). The transition from space-charge limited emission to production-limited emission is observed for ∼1 kV of effective extraction voltage (b) Detail view of the $V^{3/2}$ tendency during the space-charge limited emission, fitting the curve for 600 mA of arc current. The uncertainty of the effective voltage is ∼100 V.

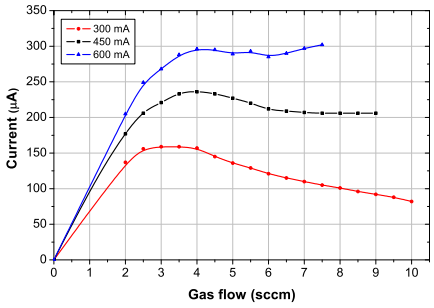

Fig. 10. Beam current measurement as a function of the gas flow rate for different arc current. The effective extraction voltage was fixed at 2.5 kV.

during the measurements, that is to say, the ion source parameters and the beam current do not present exactly the same values, even though the trend of these magnitudes remains unaltered. However, their influence on the final outcomes is limited by the carefully systematic method of measurements employed during the measurements.

It is important to comment that the extractions conditions at the IST are different from the extraction scheme in the cyclotron. In the first case, the extraction is performed by DC voltage by means of a movable puller that allowed adjusting the gap distance before the operation to maximize the beam extraction while avoiding electric sparks. In these conditions, the gap was set to the closest distance of about 3 ± 1 mm, implying a static electric field of ∼1.7 MV/m. The uncertainty in the gap measurement was severely restricted due to limited accessibility to this specific area on the test bench. In the scenario of the cyclotron operation, the extraction electric field is oscillating at the frequency of the RF resonant cavity, 60 MHz, providing a 60 kV accelerating peak voltage in the 6 mm extraction gap. Besides that, the reduced dimensions of the central region of the cyclotron imposed by the high magnetic field lead to high electric fields at the peak of the RF cycle close to 10 MV/m in the first stages at the source exit. Consequently, the ion source is expected to work in the production emission regime during the cyclotron operation. Despite this, stagnation in the perveance curve could be expected under the high voltage conditions during the cyclotron injection because the survival of H^- ions is constrained to the surface of the plasma arc column [12]. In other words, higher penetration of the electric field lines into the source slit would not necessarily increase the beam current. Therefore, we cannot estimate the injected beam current in the cyclotron from the IST experimental data due to the different operating conditions between the IST and the AMIT cyclotron. However, such measurements provide valuable information for the validation of the design and the optimum operating settings of the ion source with independence of the beam extraction conditions considered. In particular, the arc configuration for the source kick-start, the relation of the performance with the gas flow rate as well as the beam extracted as a function of the gas flow are relevant parameters established for the final start-up of the ion source in the cyclotron.

3.3. Cathode lifetime influence

The cathode lifetime is one of the main factors determining the total operating life of the ion source. Their deterioration is of great relevance since it diminishes the availability of the machine for radioisotope production and increases the cost associated with the replaceable material as well as increased exposure to ambient radiation. The experimental test at the IST has provided meaningful information about this issue. After many hours of ion source operation, the time needed by the ion source to reach the thermionic mode was increased, denoting the wear of the cathodes. When the material wear was extremely high, the ion source could not be turned on. The removal and replacement of the cathodes revealed an important erosion of the surface, with a misalignment of one of them (Fig. 11). The sputtering of the cathodes by ions from the discharge produces a crater-shaped erosion profile. The lifetime at the moment of the replacement was 23.57 A · h, a value that takes into account both the operational time and the supported current during this time because the arc discharge current determines the hit of the electrons and the material erosion. The high wear during the tests was produced because the ion source was operated close to the performance limits of the arc discharge at high arc currents.

The effect of cathode wear is studied comparing the ion source performance and the ion production for new and eroded cathodes (Fig. 12). The extracted current is affected by the wear of the cathodes, with ∼30% more current measured at the beam probe with new cathodes. Therefore, the reduction of the arc current arises as an important factor to decrease the damage of the cathodes, extending the operating life of the source.

Fig. 11. AMIT ion source cathodes after several hours of operation at the IST facility. The erosion of the surface is clearly appreciated.

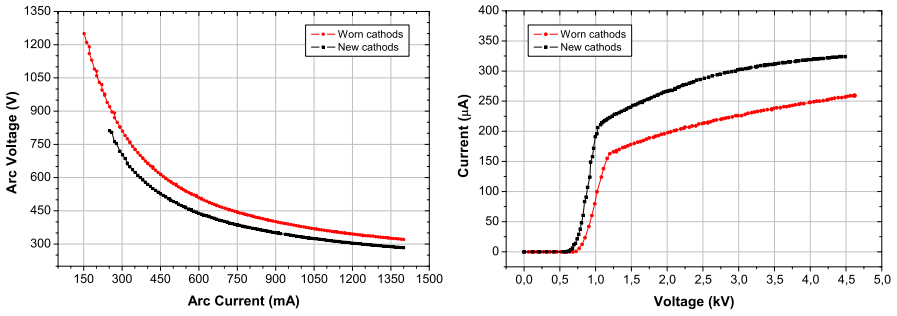

Fig. 12. Ion source characterization (a) and beam current produced (b) with new and worn cathodes for 4 sccm of gas flow rate. Beam current at the beam probe has been measured at 450 mA of arc current.

3.4. Plasma expansion gap study

A parameter evaluated during the ion source tests was the dependence between the inner anode wall and the plasma arc column. This geometric parameter influences on the H^- ions survival, modifying consequently the plasma conditions. In addition, it determines the efficiency of the electric field to extracts the ions. Hence, after some theoretical analysis and by similarity with previous studies [10,12], it was decided to manufacture three cylindrical chimneys with different plasma expansion gap distances of 0.2, 0.3 and 0.4 mm between the plasma column and the internal wall of the anode. The chimneys have equal dimension of the anode hole and the same slit size.

Fig. 13 shows the beam measurements for different chimneys employed. The results of these measures are inconclusive, since no one of the chimneys provides a clear improvement in the current extracted from the ion source under whatever operating condition. The variation of the plasma parameters has a high influence on the beam production, observable with measurements at fixed extraction voltage; even though for steady plasma conditions there is an obvious difference in the extracted current. In other words, the extracted current varies under changes in the source parameters such as the arc current and the gas flow rate in a non-reproducible way and without a clear observed trend that could be related to some physical process that justifies the measured results. Therefore, it is difficult to conclude in an optimum plasma expansion gap for the chimney. Nevertheless, in certain optimal operating conditions (4 sccm), concluded in previous section, a 0.2 mm of plasma expansion gap has provided a higher beam current during the measurements.

A relevant factor in these inconclusive results is the high uncertainty associated with the accuracy of the chimney manufacturing. This is a delicate part of small dimensions, and therefore the fine adjustment between the hole in the anode and the wall of the anode is highly complex from a technical point of view. Furthermore, it was not possible to verify after manufacturing the different distances of the plasma column, increasing the uncertainty about the real difference between the chimneys.

Summarizing, the measurements with different plasma expansion gap have not been conclusive. However, this constitutes the starting point for future studies to correct the defects observed during this experimental tests providing reliable results. Consequently, the comprehension of a real improvement base on that geometry modification depends on future measurements and analysis of the results.

3.5. Beam profile characterization

In order to characterize the beam profile, a transverse interceptive beam diagnostic based on fluorescent screen of Al_2O_3:Cr has been employed to record in situ the impact of the beam on the monitor. The device allows to measure the beam size with a 2-millimeter grid carved on it. The experimental measurements were performed at a fixed position of the screen, modifying the magnetic field, and consequently the radius of the orbits, to monitor the transition of the beam on the screen.

The results were recorded in video by a live camera installed inside the electric shield box. Fig. 14 shows a screen capture of the beam during the experiment and both transversal profiles after the post-processing of the image. The delay shine of the beam produced by fluorescence is appreciated, that is to say, the time that the screen emits light is prolonged few milliseconds, producing a visible light tail in the beam movement direction. Nevertheless, the high beam deposition, concentrated in a very small region of space, damage the device during the experiment and an area of the screen was found to be burned.

The beam profile measurements have provided relevant information to characterize the beam size produce with the AMIT internal ion

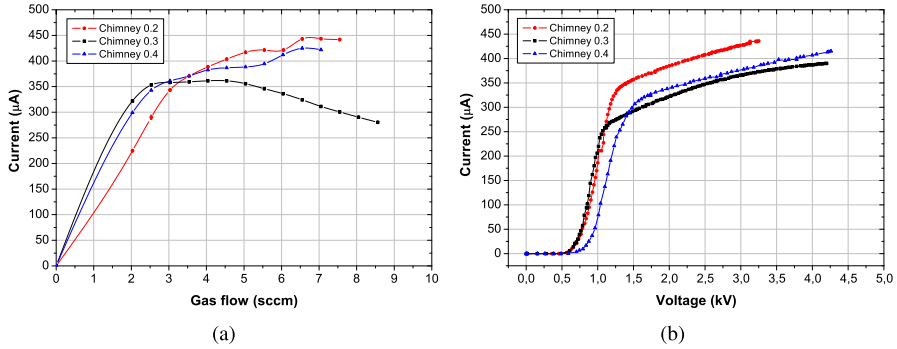

Fig. 13. Beam current at the beam probe for different chimneys with expansion gap modified as a function of (a) the gas flow rate at fixed extraction voltage (2.5 kV) and (b) in front of the effective voltage at 4 sccm of gas flow rate and 600 mA of arc current.

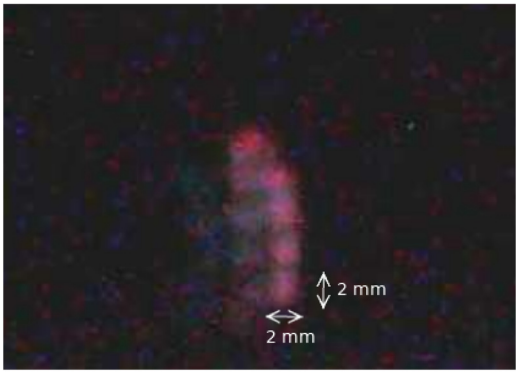

(a)

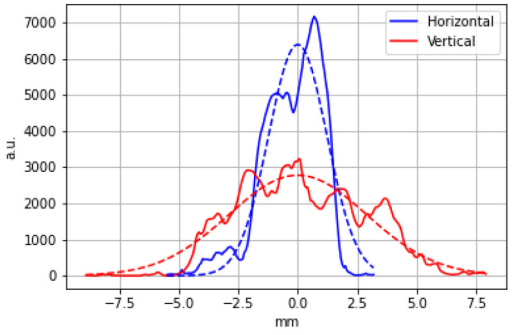

(b)

Fig. 14. Experimental measurements of the beam profile. (a) Beam profile live image from the camera. The screen emit visible light of the intercepted beam. (b) Horizontal and vertical transverse beam profiles obtained by post-processing of the image with a calibration factor of 0.15 mm/pixel. The dashed line represent a Gaussian fit to the profiles.

source. Future implementations of the IST facility will allow a better characterization of the beam through some enhancements of the beam acquisition as well as a robust monitoring of the extraction control parameters. In this way, the beam extraction will be able to be reproduced computationally through multiparticle simulations performed with a beam dynamics code to verify the experimental results.

4. Conclusion

The measurements performed at the IST have provided significant knowledge to establish a procedure for operation of the AMIT ion source. First, the discharge characteristics of the baseline configuration of the cold cathode PIG ion source has been studied at different conditions. Thus, the designed ion source have been validated for its deployment in the cyclotron, establishing the configuration for a well-suited starting point of the source as well as the dependence with internal parameters. Secondly, the beam current have been measured under different extraction conditions, varying the operation conditions of the ion source. This results will allow establishing an optimum range of the ion source control settings. Furthermore, different anode geometry modifying the plasma expansion gap have been studied. Additionally, the experimental operation has given relevant information to optimize the ion source design at a mechanical level, as well as to correct certain defects identified in the facility. Last but not the least, the beam profile has been measured and characterized by a dedicated on-site beam diagnostic, as well as it has been validated with beam dynamics simulations performed with OPAL code.

CRediT authorship contribution statement

Pedro Calvo: Formal analysis, Validation, Investigation, Writing – original draft, Writing – review editing, Visualization. **Diego Obradors:** Formal analysis, Validation, Investigation, Writing – review editing. **Rodrigo Varela:** Formal analysis, Investigation, Writing – review editing. **Iván Podadera:** Investigation, Writing – review editing. **Concepción Oliver:** Methodology, Investigation, Writing – review editing. **Antonio Estévez:** Software, Data curation. **Manuel Domínguez:** Resource, Validation. **Cristina Vázquez:** Software, Resources, Data curation, Validation. **Fernando Toral:** Project administration, Conceptualization, Supervision. **Luis García-Tabarés:** Project administration, Conceptualization, Funding acquisition. **José Manuel Pérez:** Project administration, Funding acquisition.

Declaration of competing interest

The authors declare that they have no known competing financial interests or personal relationships that could have appeared to influence the work reported in this paper.

Acknowledgment

This work was partially supported by the Spanish Ministry of Economy and Competitiveness under projects FIS2013-40860-R and FPA2016-78987-P.

References

[1] The Supply of Medical Radioisotopes. 2019 Medical isotope demand and capacity projection for the 2019–2024 period, Technical Report NEA/SEN/HLGMR(2019)1, Nuclear Energy Agency (NEA), 2019, OECD Publishing.
[2] U. Zetterberg, Compact Accelerators for Isotope Production, Cockcroft Institute, Daresbury, UK, 2015.
[3] V. Smirnov, Phys. Part. Nuclei 47 (5) (2016) 863–883.
[4] The Supply of Medical Isotopes: an Economic Diagnosis and Possible Solutions, Technical Report, Nuclear Energy Agency (NEA), 2019, OECD Publishing.
[5] Cyclomed Technologies SL, 2019, http://cyclomed.tech/es.
[6] C. Oliver, et al., in: Proceedings of the 20th International Conference on Cyclotrons and their Applications, CYC 2013, Vancouver, BC, Canada, 2013, pp. 429–431.
[7] L. García-Tabaré, et al., IEEE Trans. Appl. Supercond. 26 (4) (2016) 1–4.
[8] J. Munilla, et al., IEEE Trans. Appl. Supercond. 26 (3) (2016) 1–4.
[9] D. Gavela, et al., in: Proceedings of the 6th International Particle Accelerator Conference, IPAC 2015, Richmond, Virginia, USA, 2015, pp. 3055–3057.
[10] D.H. An, I.S. Jung, J. Kang, H.S. Chang, B.H. Hong, S. Hong, M.Y. Lee, Y. Kim, T.K. Yang, J.S. Chair, Rev. Sci. Instrum. 79 (2008) 02A520.
[11] Z. Yang, P. Dong, J. Long, T. Wang, C. Lan, Y. Peng, T. Wei, X. He, K. Zhang, J. Shi, Nucl. Instrum. Methods Phys. Res. A 685 (2012) 29–34.
[12] T.Y.T. Kuo, G.O. Hendry, in: Proceedings of the 20th International Conference on Cyclotrons and their Applications, CYC 2013, Vancouver, BC, Canada, 2013, pp. 352–356.
[13] S. Silakhuddin, S. Santosa, Atom Indones. 41 (3) (2015) 139–143.
[14] S.R. Lawrie, D.C. Faircloth, A.P. Letchford, M.O. Whitehead, T. Wood, Rev. Sci. Instrum. 87 (2016) 02B122.
[15] G.J. Schulz, Phys. Rev. 113 (3) (1959) 816–819.
[16] K. Prelec, T. Sluyters, Rev. Sci. Instrum. 44 (10) (1973) 1451–1463.
[17] R.K. Janev, D. Reiter, U. Samm, Collision Processes in Low-Temperature Hydrogen Plasmas, Technical Report Jül-4105, Forschungszentrum Jülich, Germany, 2003.
[18] C.L. Lykke, K.K. Murray, W.C. Lineberger, Phys. Rev. A 43 (11) (1991) 6104.
[19] D. Obradors, et al., in: Proceedings of the 8th International Particle Accelerator Conference, IPAC 2017, Copenhagen, Denmark, 2017, pp. 1740–1742.
[20] ANTEC SAU, 2020, https://antec-group.com/.
[21] R. Varela, et al., in: Proceedings of the 5th International Beam Instrumentation Conference, IBIC 2016, Barcelona, Spain, 2016, pp. 108–110.
[22] L. Spitzer, Physics of Fully Ionized Gases, Second ed., Interscience Publisher, 1957.
[23] C.D. Child, Phys. Rev. (Series I) 32 (5) (1911) 492–511.
[24] I. Langmuir, Phys. Rev. 2 (6) (1913) 450–486.